

# A Wideband Wide-Angle Ultra-Thin Metamaterial Microwave Absorber

Deepak Sood\* and Chandra Charu Tripathi

**Abstract**—A novel design of wideband, ultra-thin, wide-angle metamaterial microwave absorber has been presented. The unit cell of the proposed structure is designed by using parametric optimization in such a way that absorption frequencies come closer and give wideband response. For normal incidence, the simulated FWHM bandwidth of the proposed structure is 1.94 GHz, i.e., from 5.05 GHz to 6.99 GHz and  $-10$  dB absorption bandwidth is 1.3 GHz from 5.27 GHz to 6.57 GHz. The proposed structure has been analyzed for different angles of polarization, and it gives high absorption (more than 50%) for oblique angles of incidence up to  $60^\circ$ . The designed absorber is in low profile with a unit cell size of  $\lambda_0/6$  and ultrathin with a thickness of  $\lambda_0/32$  at the center frequency of 5.92 GHz corresponding to 10dB absorption bandwidth. The current and electromagnetic field distributions have been analyzed to understand the absorption mechanism of the absorber. An array of the proposed absorber has been fabricated and experimentally tested for various polarization angles and oblique incidences of electromagnetic wave. The proposed absorber is well suited for surveillance and other defense applications.

## 1. INTRODUCTION

A perfect microwave absorber is an electromagnetic device which can absorb incident radiations with minimum reflection and transmission [1]. Conventional absorbers such as Salisbury [2] and Dallenbach absorbers [3] have narrowband and are electrically thick. From the last decade, due to the exotic properties of metamaterials at subwavelength scale they are in continuous use for the performance improvement of microwave absorbers [4]. The ultra-thin thickness and nearly unity absorbance property of a metamaterial based absorber make it a useful candidate from microwave to optical frequencies in many potential applications such as cloaking [5], antennas [6], radar imaging [7], thermal emission [8, 9] photodetector [10], solar cells [11], etc. Metamaterial absorbers are so designed that incident electromagnetic energy on the structure manipulate its effective permittivity and permeability in such a way that input impedance of the structure become equals to the free space impedance and minimizes the reflection from it.

Due to strong, simultaneous electric and magnetic resonance at a particular frequency, the metamaterial based absorbers suffer from narrow bandwidth, which limits their practical applications. So far, most of the metamaterial absorbers are designed for dual band [12–14], triple band [15] and multiband [16] operations. Based on the concept of multiple resonances, a few monolayer designs with moderate enhancement in bandwidth have been proposed [17, 18]. They are complicated in design, and it is cumbersome to control the individual resonance frequencies in these multi-resonant structures. Bandwidth enhanced absorbers based on the concept of combining different resonant structures have also been presented in [19–21]. Although this approach enhances the bandwidth, it increases the overall size of unit cell which limits its practical applications. Another approach for a bandwidth enhanced

---

*Received 29 August 2015, Accepted 29 September 2015, Scheduled 7 October 2015*

\* Corresponding author: Deepak Sood (deepaksood.uiet@gmail.com).

The authors are with the Department of Electronics & Communication Engineering, University Institute of Engineering & Technology, Kurukshetra University, Kurukshetra (Haryana), India.

absorber involves the use of vertically stacked multiple layers [22, 23]. This vertical stacking of layers increases the overall thickness of the structure, which limits its conformal planar applications. Recently, an ultra-wideband ultrathin metamaterial absorber has been proposed in [24] with a thickness of  $\lambda_0/15$ . Although it covers entire X-band, its thickness is still large at the operating frequency.

In this paper, a novel design of planar, wideband, ultrathin metamaterial microwave absorber has been presented. Four circular slots have been constituted symmetrically w.r.t center of the unit cell on the top hexagonal metallic layer. Circular slots provide resonance at lower frequency and hexagonal metallic patch gives high frequency resonance with considerable increase in bandwidth. The radii of the circular slots and dimensions of hexagonal patch have been varied to observe their contributions to wideband absorption. The proposed structure exhibits more than 90% absorption from 5.27 GHz to 6.57 GHz. Analysis of field and surface current distribution is performed to better understand the absorption mechanism. The proposed structure has been investigated for different oblique angles of incidence of EM wave and for various polarization angles under normal incidence. An array of the proposed design has been fabricated using MITS milling machine, and experimental results are in good agreement with the simulated responses. In comparison to metamaterial absorbers presented so far, the proposed absorber is ultra-thin with a thickness of  $\lambda_0/32$ .

## 2. DESIGN AND SIMULATION

The design of unit cell of the proposed ultrathin wideband absorber is shown in Fig. 1(a). In the unit cell, top metal patch and bottom ground plane are separated by a dielectric FR-4 substrate ( $\epsilon_r = 4.4$  and  $\tan \delta = 0.02$ ) with thickness ( $h$ ) of 1.6 mm. The top metal layer is etched at the top left and bottom right corner (hexagon shape), and it is constituted with four circular slots of equal radii. The top and bottom metal planes are made of copper with thickness 0.035 mm and conductivity  $\sigma = 5.8 \times 10^7$  S/m. The optimized geometric dimensions are as follows:  $L = 5.8$  mm,  $D = 3.0$  mm and  $S = 1.9$  mm. The absorption coefficient is computed as  $A = 1 - |S_{21}|^2 - |S_{11}|^2$ . Here  $|S_{21}|^2$  and  $|S_{11}|^2$  are transmitted and reflected powers, respectively. As the back plate is copper, there is no transmission of power and therefore  $|S_{21}|^2 = 0$ . Thus absorption can be calculated as:  $A = 1 - |S_{11}|^2$ .

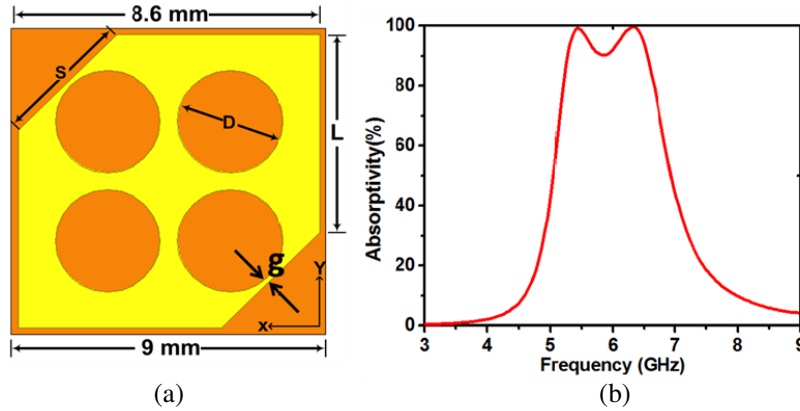


**Figure 1.** (a) Front view of proposed unit cell, (b) simulated absorptivity under normal incidence.

For the analyses of the proposed absorber, unit cell is simulated with Floquet's periodic boundary conditions using ANSYS HFSS. The simulated response for normal incidence of plane wave onto the proposed absorber is shown in Fig. 1(b). It is observed that the FWHM bandwidth is 1.94 GHz, (5.05 GHz to 6.99 GHz), which covers 49% of C band. The proposed absorber shows more than 90% absorption from 5.27 GHz to 6.57 GHz, which is 33% of C band. There are two absorption peaks at  $f_1 = 5.34$  GHz and  $f_2 = 6.33$  GHz with absorption rates of 99.20% and 99.62%, respectively.

Further, in order to analyze the polarization behaviour, the proposed absorber has been investigated for different polarization angles as shown in Fig. 2(a). It is observed that the proposed structure is two-fold symmetric, i.e., as the polarization angle increases, absorption decreases. After  $45^\circ$ , it

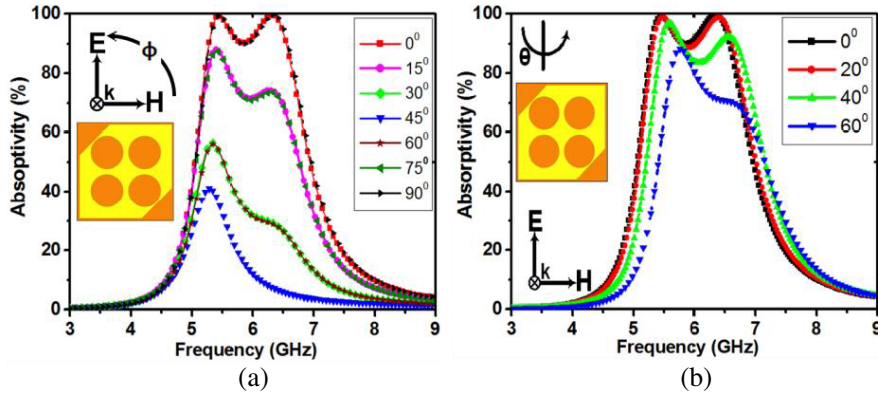


**Figure 2.** (a) Simulated absorptivity (a) for different polarization angles ( $\phi$ ) under normal incidence, (b) for different incidence angles ( $\theta$ ) under TE polarization.

again increases and becomes maximum at  $90^\circ$  which is in accordance with observation reported in [24]. The proposed absorber has also been studied for various oblique angles of incident wave under TE polarization from  $0^\circ$  to  $60^\circ$  in the intervals of  $20^\circ$  as shown in Fig. 2(b). It is seen that as incident angle increases, both the absorption peaks start shifting toward higher frequencies. The second absorption peak decreases in magnitude and gradually disappears at  $60^\circ$ . Moreover, it is also observed that up to the incident angle of  $40^\circ$ , the absorption is more than 90% from 5.45 GHz to 6.67 GHz with a  $-10$  dB bandwidth of 1.22 GHz. At the incident angle of  $60^\circ$ , the FWHM absorption bandwidth is 1.73 GHz (5.42 GHz to 7.15 GHz). Therefore, the proposed absorber provides high absorption for the wide incident angles.

### 3. RESULTS AND DISCUSSIONS

In order to verify the absorption properties of the proposed ultrathin wideband microwave absorber, a prototype consisting of  $20 \times 20$  unit cells has been fabricated (by using microstrip milling machine of MITS, Japan) as shown in Fig. 3(a). An enlarged view of a portion of fabricated structure is shown in Fig. 3(b). The prototype is fabricated on an FR-4 substrate with a thickness of 1.6 mm as that used for numerical simulations. Testing of the prototype was performed as suggested in [19–22, 24]. Two UWB horn antennas (VSWR  $< 2$ , over 1 to 18 GHz of frequency range) connected to Agilent’s vector network analyzer (model No. N5222A) are used. One antenna is used as transmitting antenna, and the other is used as a receiving antenna.

In the first step, calibration of the testing setup was performed by measuring the reflection coefficient of an identical copper sheet placed at a distance at which near-field effects are negligible from the UWB horn antennas. Then, reflection coefficient of the fabricated structure was measured for normal

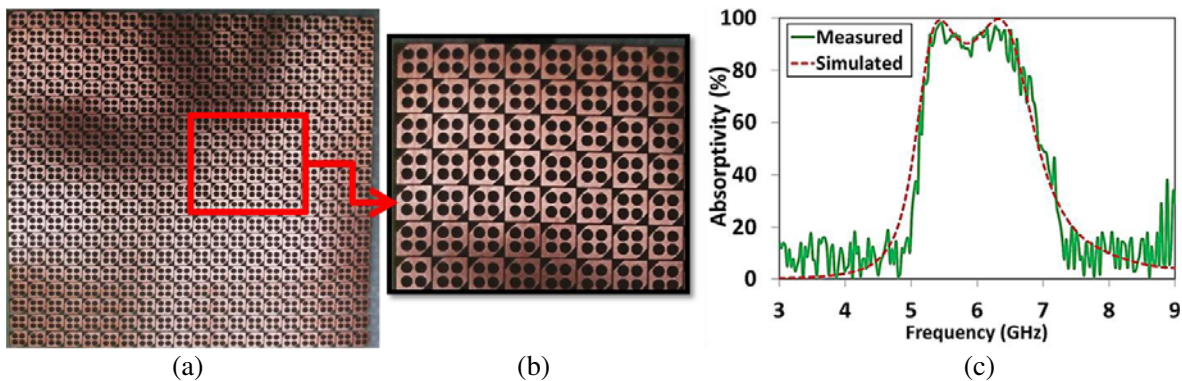


**Figure 3.** (a) Fabricated structure, (b) enlarged view, (c) comparison of simulated and measured absorptivity.

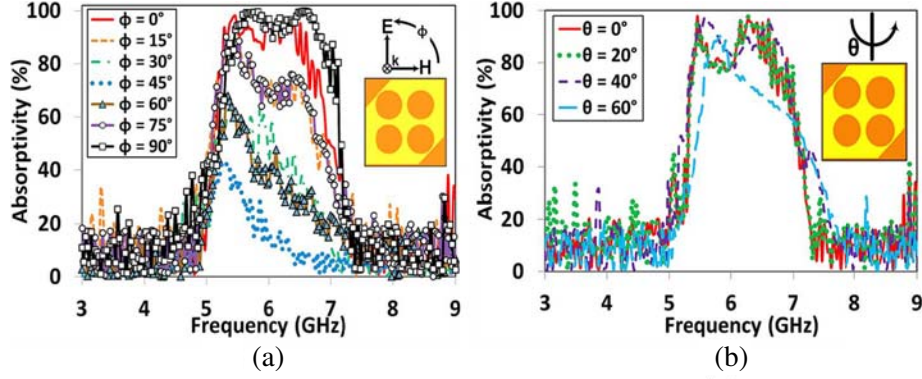


**Figure 4.** Measured absorptivity for (a) different polarization angles under normal incidence and for (b) different oblique incidence angles under TE polarization.

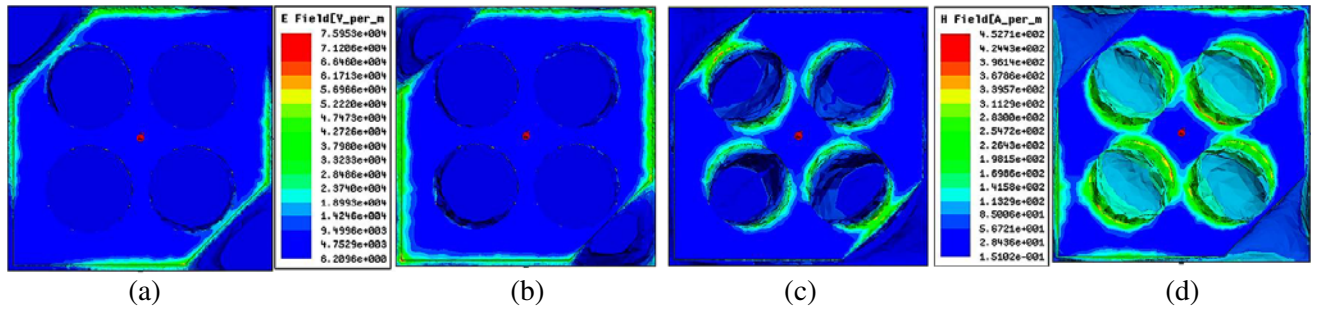


**Figure 5.** Electric field distribution at (a) 5.43 GHz and (b) 6.33 GHz and magnetic field distribution at (c) 5.43 GHz and (d) 6.33 GHz.

incidence by replacing the copper sheet with fabricated sample. Thereafter, the difference between the two measured results was obtained, which gives the actual reflection ( $S_{11}$ ) from the fabricated prototype. From  $S_{11}$  values, absorption ( $A$ ) is evaluated, and the comparison of simulated and measured results is shown in Fig. 3(c).

The fabricated sample has also been tested for different angles of polarization from  $0^\circ$  to  $90^\circ$ , and the measured absorption is as shown in Fig. 4(a). It is observed that the measured absorption response is in agreement with the simulated one, i.e., absorption decreases as polarization angle increases up to  $45^\circ$ , and it increases again as angle increases up to  $90^\circ$ . Further, the measured absorption at different angles of incidence ( $0^\circ$  to  $60^\circ$ ) of the incident wave for TE polarization is shown in Fig. 4(b). Transmitting and receiving antennas are positioned at oblique angles, along the circumference of a circle at the center where fabricated prototype is placed, and the radius of the circle is equal to the distance at which near-field effects are minimum. The measured and simulated results are in good agreement as it is observed that for higher incident angles, the proposed absorber provides higher absorption with wideband response. It is also evident that the second absorption peak disappears at  $60^\circ$ , same as in simulated response.

Now, in order to better understand the absorption phenomenon at the two absorption peaks, i.e., 5.43 GHz and 6.33 GHz, the simulated field (electric and magnetic) distributions have been illustrated in Fig. 5. In a metamaterial based absorber, the top metallic periodic structure is electrically excited while the dielectric substrate is excited by the incident magnetic field as explained in [1]. In the proposed absorber, at the lower absorption frequency of 5.43 GHz, the electric and magnetic couplings are clearly evident across the gap ‘ $g$ ’ between the etched corners (top left and bottom right) and the circular slots as shown in the Fig. 5(a) and Fig. 5(c), respectively. This strong electromagnetic coupling is mainly responsible for high absorption according to the theory explained in [25]. At the higher resonance frequency of 6.33 GHz, outer edge (having dimension ‘ $L$ ’) of the structure is the main contributor; however, four circular slots contribute high magnetic resonance at this frequency due to high dielectric loss. The magnetic field coupling is also observed in the intermediate region between the adjacent

circular slots.

The surface current distribution at the two absorption peaks has been illustrated in Fig. 6. Although there is a good amount of current flowing in all parts of the unit cell which proves strong magnetic resonance in the structure, it is observed that at lower absorption frequency, the surface current is mainly distributed across the gap ‘*g*’ between the etched corners and the edges of the circular slots. For high frequency resonance, the current is mainly distributed at the edge of dimension ‘*L*’ and the circumference of the circular slots. The surface currents are antiparallel at the top and bottom surfaces for both the resonance frequencies thereby form a counter-circulating loop driven by the incident magnetic field. These antiparallel currents create a strong magnetic excitation in the structure similar to the fishnet structure as reported in literature [26]. The simultaneous appearance of electric and magnetic excitations at the resonance frequencies of 5.43 GHz and 6.33 GHz is supposed to result in high absorption of incident electromagnetic field in the proposed absorber.

Further, to understand the contribution of various design parameters in the absorption bandwidth, parametric analyses have been performed for normal incidence. As the etched corners are the main contributors in the absorption, the variations in their slanting length ‘*S*’ has been studied by varying parameter ‘*L*’ as shown in Fig. 7(a). It is observed that as ‘*L*’ increases (i.e., as the slanting length ‘*S*’ of the etched corners decreases), the first resonance frequency remains unchanged, but the second resonance frequency decreases. This results in the reduction in bandwidth. The second resonance frequency (*f*<sub>2</sub>) disappears at ‘*L*’ = 6.7 mm. Absorption bandwidth for different values of ‘*S*’ is listed in Table 1.

Other critical parameters, which affect the absorption bandwidth, are the number and position of circular slots used and the diameter of circular slot (‘*D*’). The number of circular slots and their positions are critically optimized in the proposed design, as the geometric dimensions, position, orientation and number of resonant elements in the unit cell of a metamaterial based absorber largely affect the absorption bandwidth in accordance with observation reported in literature [12, 15, 20, 21

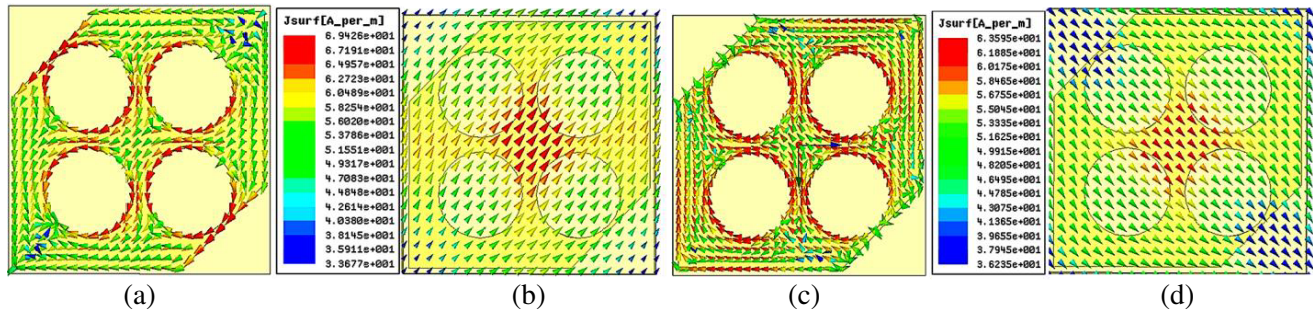


**Figure 6.** Surface current distribution at 5.43 GHz (a) top surface, (b) bottom surface and at 6.33 GHz (c) top surface, (d) bottom surface.

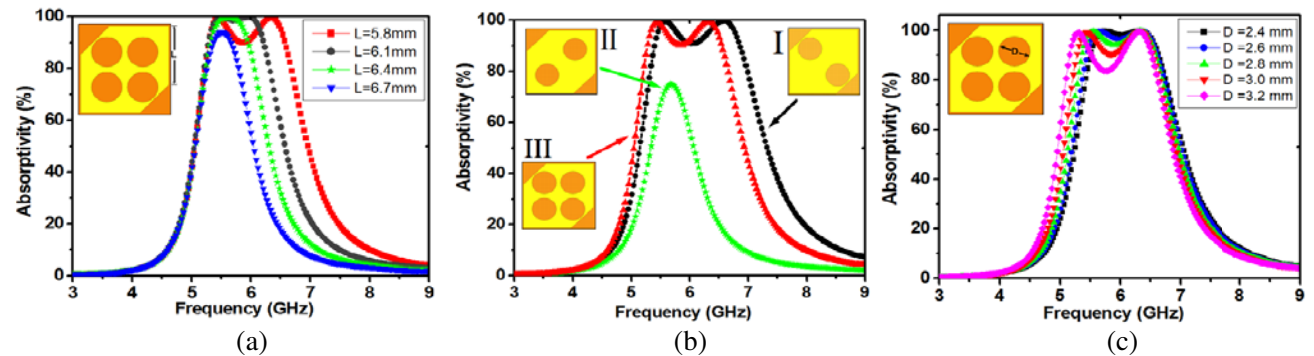


**Figure 7.** Simulated absorption (a) for different values of ‘*L*’ of hexagonal patch, (b) for different positions of circular slots, (c) for different diameters of circular slots.

& 24]. In the proposed absorber, it is observed that with two circular slots in position-I as shown in Fig. 7(b), the  $-10$  dB bandwidth is 1.44 GHz (5.41–6.85) GHz and FWHM bandwidth 2.22 GHz (5.12–7.34) GHz, and for the position-II, the  $-10$  dB bandwidth is nil and FWHM bandwidth merely 0.75 GHz (5.33–6.08) GHz. Thus, in position-I, the placement of circular slots near the etched corners enhances the electromagnetic coupling across the gap ‘ $g$ ’ which is responsible for providing high absorption over wideband. For position-III,  $-10$  dB bandwidth is 1.3 GHz (5.27–6.57) GHz and FWHM bandwidth 1.94 GHz (5.05–6.99) GHz. The presence of additional circular slots as in position-III results in the electromagnetic coupling between adjacent circular slots as evident in field and surface current distribution. This shifts both absorption peaks towards low frequency side and provides an effective mean to control the absorption bandwidth.

The contribution of the diameter of the circular slots in the absorption bandwidth has also been investigated as shown in Fig. 7(c). It is observed that as diameter increases, the second resonance frequency ( $f_2$ ) remains unchanged, but the first resonance frequency ( $f_1$ ) gradually decreases, which results in the increase in absorption bandwidth. Absorption is maximum and more than 90% for  $D = 3.0$  mm with a bandwidth equals to 1.3 GHz. For the further increase in diameter, i.e.,  $D = 3.2$  mm, the gap between circular slots and etched corners becomes negligibly small, which reduces the first resonance frequency ( $f_1$ ) to a large extent. This causes a large separation between two absorption peaks ( $f_1$  &  $f_2$ ) with  $-10$  dB absorption bandwidth approaching nil. At the diameter of 3.2 mm, the proposed structure provides two absorption peaks at 5.30 GHz and 6.30 GHz with a bandwidth of 1.53 GHz (5.09–6.62 GHz) and more than 80% absorption. Absorption bandwidth for different values of ‘ $D$ ’ is listed in Table 2. The proposed absorber has been compared with the pervious metamaterial based absorbers in Table 3. It is observed that the designs in [18] and [20] are electrically thin compared to proposed one, but they have less FWHM bandwidth and larger unit cell size. Further, the design proposed in [17] has small unit cell size with electrically thin thickness, but its FWHM bandwidth is less than the proposed work. Although [24] has higher FWHM bandwidth than the proposed absorber, it does not support wide angle absorptivity, and its thickness is large.

Therefore, the proposed design is in low profile with its unit cell size of  $\lambda_0/6$ , ultra-thin with a thickness of  $0.031\lambda_0$  and gives wideband with a FWHM bandwidth of 1.94 GHz, i.e., 32.77% at the center frequency of 5.92 GHz, which makes it suitable for applications which require compact, thin and wideband absorbers for larger incident angle such as cloaking, antennas and phase imaging.

**Table 1.** Absorption bandwidth for different values of slant length ‘ $S$ ’.

S. No.	L (mm)	S (mm)	$f_1$ (GHz)	$f_2$ (GHz)	FWHM Bandwidth (GHz)	$-10$ dB Bandwidth (GHz)
1	5.8	3.96	5.34	6.33	1.94	1.30
2	6.1	3.54	5.49	5.97	1.54	0.94
3	6.4	3.11	5.50	5.74	1.27	0.64
4	6.7	2.68	5.55	Nil	1.01	0.31

**Table 2.** Absorption bandwidth for different values of diameter ( $D$ ) of circular slots.

S. No.	D (mm)	$f_1$ (GHz)	$f_2$ (GHz)	FWHM Bandwidth (GHz)	$-10$ dB Bandwidth (GHz)
1	2.4	5.73	6.33	1.83	1.13
2	2.6	5.64	6.36	1.86	1.17
3	2.8	5.55	6.33	1.87	1.22
4	3.0	5.34	6.33	1.94	1.30
5	3.2	5.30	6.30	1.95	Nil

**Table 3.** Comparison of proposed absorber with previous metamaterial absorbers.

Absorber	Center Frequency (GHz)	Unit Cell Size mm	Thickness mm	FWHM Bandwidth (GHz)
[17]	9.98	7.2	1.0 ( $0.033\lambda_0$ )	11.52%
[18]	10.0	14.2	0.6 ( $0.02\lambda_0$ )	11.0 %
[19]	10.23 (at X-band)	18.0	1.0 ( $0.034\lambda_0$ )	9.43%
[20]	5.15	10.0	1.0 ( $0.017\lambda_0$ )	8.13%
[21]	10.38	10.0	1.0 ( $0.034\lambda_0$ )	6.55%
[22]	6.90 (at C-band)	20.0	3.2 ( $0.073\lambda_0$ )	21.40%
[24]	10.05	7.1	2.0 ( $0.067\lambda_0$ )	72.64%
Proposed Absorber	5.92	9.0	1.6 ( $0.031\lambda_0$ )	32.77%

#### 4. CONCLUSION

A wideband ultra-thin metamaterial based microwave absorber has been presented. The simulation results show above 90% absorption with a bandwidth of 1.3 GHz, ranging from 5.27 GHz to 6.57 GHz, and FWHM bandwidth is 1.94 GHz (5.05 to 6.99) GHz. Simulated results are in good agreement with the measured ones. To better understand the absorption phenomenon electromagnetic field and surface current distributions have been illustrated. Essential design parameters are critically analyzed to investigate the wideband response of the proposed absorber. The performance of the proposed absorber has also been experimentally investigated for polarization dependence and for different incident angles. Compared to the existing metamaterial based absorbers, the proposed absorber is wideband for large incident angles, ultra-thin and in low profile. Therefore, it can be used for cloaking, antennas, phase imaging, RCS reduction and other defense applications in C-band.

#### ACKNOWLEDGMENT

We acknowledge the support of Mr. Saptarishi Ghosh (Ph.D. Scholar), Department of Electrical Engineering, IIT, Kanpur, India for valuable discussions regarding the measurements of the fabricated samples. The work is financially supported by TEQIP-II (sub-component 1.1) — a World Bank assisted project.

#### REFERENCES

1. Landy, N. I., S. Sajuyigbe, J. J. Mock, D. R. Smith, and W. J. Padilla, "Perfect metamaterial absorber," *Phys. Rev. Lett.*, Vol. 100, 207402, 2008.
2. Chambers, B., "Optimum design of a salisbury screen radar absorber," *Electron. Lett.*, Vol. 30, 1353–1354, 1994.
3. Salisbury, W. W., "Absorbent body of electromagnetic waves," United States Patent 2,599,944, June 10, 1952.
4. Smith, D. R., W. J. Padilla, D. C. Vier, S. C. Nemat-Nasser, and S. Schultz, "Composite medium with simultaneously negative permeability and permittivity," *Phys. Rev. Lett.*, Vol. 84, 4184–4187, 2000.
5. Schurig, D., J. J. Mock, B. J. Justice, S. A. Cummer, J. B. Pendry, A. F. Starr, and D. R. Smith, "Metamaterial electromagnetic cloak at microwave frequencies," *Science*, Vol. 314, 977–980, 2006.
6. Enoch, S., G. Tayeb, and P. Vincent, "A metamaterial for directive emission," *Phys. Rev. Lett.*, Vol. 89, 3901–3904, 2002.

7. Fallahi, A., A. Yahaghi, H. R. Benedickter, H. Abiri, M. Sarabandi, and C. Hafner, "Thin wideband radar absorbers," *IEEE Trans. Antennas Propag.*, Vol. 58, 4051–4058, 2010.
8. Puscasu, I. and W. L. Schaich, "Narrow-band, tunable infrared emission from arrays of microstrip patches," *Appl. Phys. Lett.*, Vol. 92, 233102, 2008.
9. Liu, X., T. Starr, A. F. Starr, and W. J. Padilla, "Infrared spatial and frequency selective metamaterial with near-unity absorbance," *Phys. Rev. Lett.*, Vol. 104, 207403, 2010.
10. Rosenberg, J., R. V. Shenoi, S. Krishna, and O. Painter, "Design of plasmonic photonic crystal resonant cavities for polarization sensitive infrared photodetectors," *Appl. Phys. Lett.*, Vol. 95, 161101, 2009.
11. Hao, J., J. Wang, X. Liu, W. J. Padilla, L. Zhou, and M. Qiu, "High performance optical absorber based on a plasmonic metamaterial," *App. Phys. Lett.*, Vol. 96, 251104, 2010.
12. Li, M. H., H.-L. Yang, X.-W. Hou, Y. Tian, and D.-Y. Hou, "Perfect metamaterial absorber with dual bands," *Progress In Electromagnetics Research*, Vol. 108, 37–49, 2010.
13. Lee, H.-M. and H. Lee, "A dual band metamaterial absorber based with resonant-magnetic structures," *Progress In Electromagnetics Research Letters*, Vol. 33, 1–12, 2012.
14. Ghosh, S., D. Sarkar, S. Bhattacharyya, and K. V. Srivastava, "Design of an ultra-thin dual band microwave metamaterial absorber," *6th Annual Conf., ATMS*, 38–41, Kolkata, India, 2013.
15. Bhattacharyya, S. and K. V. Srivastava, "Triple band polarization independent ultra-thin metamaterial absorber using electric field driven LC resonator," *Journal App. Phys.*, Vol. 115, 064508, 2014.
16. Park, J. W., P. V. Tuong, J. Y. Rhee, K. W. Kim, W. H. Jang, E. H. Choi, L. Y. Chen, and Y. P. Lee, "Multi-band metamaterial absorber based on the arrangement of donut-type resonators," *Opt. Exp.*, Vol. 21, 9691–9702, 2013.
17. Ghosh, S., S. Bhattacharyya, Y. Kaiprath, and K. V. Srivastava, "Bandwidth enhanced polarization insensitive microwave metamaterial absorber and its equivalent circuit model," *Journal App. Phys.*, Vol. 115, 104503, 2014.
18. Lee, J. and S. Lim, "Bandwidth-enhanced polarization insensitive microwave metamaterial absorber using double resonance," *Electron. Lett.*, Vol. 47, 8–9, 2011.
19. Bhattacharyya, S., S. Ghosh, and K. V. Srivastava, "Triple band polarization independent ultra-thin metamaterial absorber with bandwidth enhancement at X-band," *Journal App. Phys.*, Vol. 115, 094514, 2013.
20. Bhattacharyya, S., S. Ghosh, and K. V. Srivastava, "Bandwidth-enhanced metamaterial absorber using electric field driven LC resonator for airborne radar applications," *Microw. Opt. Techno. Lett.*, Vol. 55, 2131–2137, 2013.
21. Ghosh, S., S. Bhattacharyya, and K. V. Srivastava, "Bandwidth enhancement of an ultrathin polarization insensitive metamaterial absorber," *Microw. Opt. Techno. Lett.*, Vol. 56, 350–355, 2014.
22. Bhattacharyya, S., S. Ghosh, D. Chaurasiya, and K. V. Srivastava, "Bandwidth-enhanced dual-band dual-layer polarization-independent ultra-thin metamaterial absorber," *Appl. Phys. A*, Vol. 118, 207–215, 2014.
23. Jaradat, H. and A. Akyurtlu, "Infrared (IR) absorber based on multiresonant structures," *IEEE Trans. Antennas Propag. Lett.*, Vol. 11, 1222–1225, 2012.
24. Ghosh, S., S. Bhattacharyya, D. Chaurasiya, and K. V. Srivastava, "An ultrawideband ultrathin metamaterial absorber based on circular split rings," *IEEE Trans. Antennas Propag. Lett.*, Vol. 14, 1172–1175, 2015.
25. Ghosh, S. and K. V. Srivastava, "An equivalent circuit model of FSS-based metamaterial absorber using coupled line theory," *IEEE Antennas Wireless Propag. Lett.*, Vol. 14, 511–514, 2015.
26. Kafesaki, M., I. Tsiapa, N. Katsarakis, T. Koschny, C. M. Soukoulis, and E. N. Economou, "Left-handed metamaterials: The fishnet structure and its variations," *Phys. Rev. B*, Vol. 75, 235114, 2007.